Reprinted from ENGINEERING FOR POWER, *Vol. 101, No. 4, October 1979*

Krishna P. Singh
President & CEO
Holtec International
Marlton, NJ

On Thermal Expansion Induced Stresses in U-Bends of Shell-and-Tube Heat Exchangers

An analytical method is herein developed to evaluate the stress field in the critical regions of a U-tube subject to differential thermal expansion. The solution is intended to be used as a design tool to conveniently study the variation of geometric parameters on the U-tube stress distribution. Those design variables which have significant effects on the structural characteristics of the U-tube are identified by an in-depth study of a typical example problem. Some effective design remedies are also discussed.

1 Introduction

The tubular heat exchanger, as a device to transfer heat between two fluids at different temperatures, would be considered a natural candidate for thermal expansion related problems. Indeed thermal stresses merit careful analysis in the design of all sorts of heat transfer apparatus. In shell-and-tube exchangers, the thermal stress problem usually stems from the differential expansion between the shell and the tubes. The tubes are in (turbulent) contact with both fluids undergoing the heat transfer process, whereas the shell is in contact with the shell-side fluid only. The resultant differential expansion between the shell and the tubes, sometimes abetted by the difference in the thermal expansion coefficients of tube and shell materials, is a major source of structural problems in fixed tubesheet heat exchangers [1]. This design drawback is eliminated by resorting to the U-tube construction, wherein the longitudinal expansion of the shell is physically isolated from that of the tubes. This inherent feature of U-tube design has fostered the mistaken belief that U-tube designs are immune from axial thermal expansion problems. While the relative differential expansion between the shell and the tube bundle is eliminated as a potential design problem in the U-tube construction, the thermal problem manifests itself in the tube bundle. The straight tube segments in different tube passes are, in general, subject to different flow patterns and fluid temperatures. As a consequence the two component legs of a U-tube expand or contract by unequal amounts. Since the U-tubes are "built in" at the tubesheet for all intents and purposes, the semicircular bends at the rear end of the bundle must absorb most of the differential expansion between its adjoining legs. Often, the attendant stresses are quite high.

It should be emphasized that for most practical applications the U-tube design possesses sufficient flexibility such that the aforementioned temperature difference is not a cause for serious concern. The potential inadequacy of the U-tube develops only when the temperature changes across the exchanger are relatively large. Viewed from this perspective the situation is likely to worsen as the growing emphasis on thermal efficiency drives the operating temperature of power plants even higher. The problem is specially severe in equipment used in "regeneration" type of applications. A typical example is the steam generator blow-down heat exchanger often used in PWR designs. The main function of this exchanger is to recapture most of the enthalpy of the blow-down stream. The blow-down stream must be cooled to low enough temperatures to make it agreeable to downstream equipment (e.g. dimineralizers). On the other hand it is desirable to heat the coolant stream to as high a temperature as feasible to make it thermodynamically attractive. Thus, both shell and tube-side fluids in a blow-down exchanger are subject to large temperature changes. All prerequisites for possible overstress in the U-bends are satisfied.

Large U-bend stresses are accompanied by appreciable contact forces between the tube wall and the support baffle, specially at baffles located adjacent to the U-bends. In operations subject to a large number of thermal cycles these contact forces pose a real threat of wear and fretting damage to the tube surfaces. Axial force in the tube developed due to thermal expansion loads in the tube-to-tubesheet joint, and may be dangerous to the integrity of rolled-only joints. Furthermore, axial stress in the tubes alters their natural frequency of vibration. The influence of tube natural frequency on its stability against flow induced vibration is well known to heat exchanger engineers. These considerations exemplify the importance of the U-bend thermal stress problem. Yet despite its obvious significance, this problem has not been treated in the literature. As a result, very often it is completely overlooked in the design process.

A central theme of this paper is to develop a workable set of equations to enable direct computation of the U-bend stresses. The solu-

Contributed by the Nuclear Heat Exchanger Committee and presented at the Joint Power Generation Conference, Sept 10-14, Dallas, Texas, of THE AMERICAN SOCIETY OF MECHANICAL ENGINEERS. Manuscript received at ASME Headquarters June 23, 1978. Paper No. 78-JPGC-NE-14.

tion is devised within the framework of linear elasticity theory by employing Castigliano's First Theorem. The efficacy of the solution procedure is demonstrated in a typical exchanger problem.

The first step in the analysis is to determine the metal temperature of the legs and the U-bends. Gardner [2] has given a general technique for determining tube metal temperatures. Hence it will be assumed here that the tube metal temperatures, and hence the differential thermal expansion between the legs, δ, and change in radius of the U-bend, Δ, are known. The object now is to evaluate the stresses and displacement fields in the U-tube. The mathematical model and solution procedure are described in the following section. Practical design remedies to alleviate U-bend stresses are also pointed out and discussed in some depth. A numerical example is used to illustrate the essentials of the solution technique.

2 Analysis

Fig. 1 shows the center line of a U-tube of straight length ℓ_s and bend radius r laterally supported at a number of locations by transverse baffles. The two legs of U overhang by specified amounts S_1 and S_2 respectively beyond the last support baffles labeled as tangent line baffles (TL) in Fig. 1. Let us assume that the U-tube is subject to a temperature field such that, under free expansion, leg 1 expands by an amount δ over leg 2, and the radius of the bend increases by an amount Δ. It is intuitively apparent that the bend region would be subject to the most severe stresses. Hence it is reasonable to expect that the characteristics of the support provided by the TL baffles would be specially important. Recalling that the baffles are drilled with a certain clearance (usually in the range of .015 in. to .03 in.) it is necessary to model these support locations with a specified clearance. We now proceed to derive the necessary equations to solve the elasticity problem.

The solution procedure is best described by considering freebody of the U-bend segment including the overhang spans (Fig. 2). P is the unknown axial force developed in the legs. R represents the lateral shear. M_1 and M_2 denote the bending moments produced at the TL baffle locations 0_1 and 0_2, respectively. Let

$$M_1 = \alpha_1 K_1$$
$$M_2 = \alpha_2 K_2 \tag{1}$$

where α_1 and α_2 denote in-plane rotations of legs 1 and 2 at points 0_1 and 0_2 respectively. K_1 and K_2 are the corresponding spring constants. These spring constants represent the influence of adjacent tube spans and baffle support conditions. For baffle support modeled with a small clearance, K_i will be a highly nonlinear function of α_i. More on this will follow later in this section. At this point in the analysis, it is assumed that K_1 and K_2 are known quantities.

Referring to Fig. 2, moment equilibrium yields

$$\alpha_1 = \frac{1}{K_1}[K_2\,\alpha_2 + 2\,\mathrm{Pr} - R\,(S_1 - S_2)] \tag{2}$$

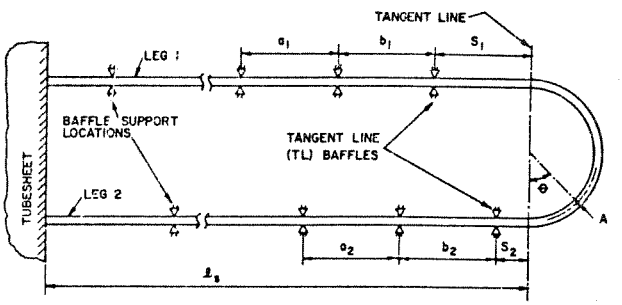

Fig. 1 U-Tube geometry

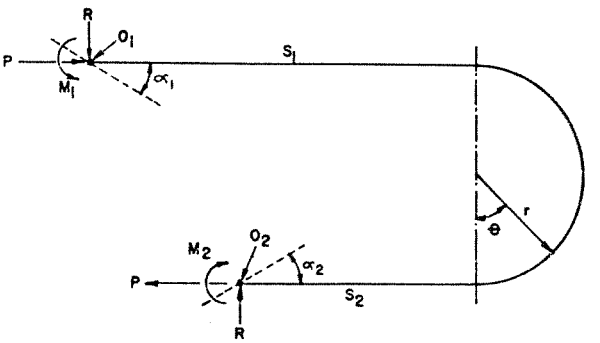

Fig. 2 Freebody of U-bend segment

To evaluate four principal unknowns in this formulation, namely α_1, α_2, P and R, three additional equations are required. We will derive these equations by appealing to a generalized form of the theorem of Castigliano [3].

We note that the gross strain energy U in the U-bend segment (Fig. 2) is given by

$$\mathrm{U} = \int \frac{N^2}{2EA}ds + \int \frac{\phi V^2}{2GA}ds + \int_{(S_1+S_2)} \frac{M^2}{2EI}ds + \int_0^{\pi} \frac{M^2\,d\theta}{2EAY_0\lambda} + \int_0^{\pi} \frac{MN}{EA}d\theta \tag{3}$$

The first two terms in the integral are contributions to the strain energy due to the axial force and shear, respectively. The integral extends over the entire length of the element. The third and fourth terms are flexural strain energy in the straight and curved segments respectively. Finally, the last term represents the contribution to the strain energy due to noncoincidence of neutral and centroidal axes in curved members. The symbols N, V and M respectively denote axial tension, lateral shear, and bending moment (positive if it in-

Nomenclature

a_i, b_i, etc. = baffle spacings (Fig. 1)
A = cross-sectional area of tube metal
C_i, C_o = inner and outer radii of tube
C_m = mean radius of tube
E = Young's Modulus of tube material
G = shear modulus of tube material
I = plane moment of inertia of tube cross section
K_i = rotation spring constant (i = 1, 2)
ℓ_s = straight length of tube leg (Fig. 1)
M = bending moment at a generic point in the U-tube
N = axial tension at a generic point in the U-tube
P = axial force
p = internal pressure
R = lateral shear at overhang baffle support locations
r = mean bend radius
S_i = overhang of leg i (i = 1, 2—Fig. 1)
t = tube wall thickness
U = gross strain energy in the freebody (Fig. 2)
V = lateral shear at a generic point in the U-tube
T_1, T_2 = support point reactions at TL baffle location (Fig. 3)
α_1, α_2 = rotation of tube legs at points 0_1 and 0_2 respectively (Fig. 2)
δ = free thermal expansion of leg 1 over leg 2 (Fig. 1)
Δ = increase in radius r of the bend due to its temperature rise
θ = angular orientation of an element in the curved region (Fig. 2)
λ = flexibility factor
ϵ_i = outward displacement of leg i at TL baffle location (Fig. 3)
ψ = stress intensification factor for the U-bend
ξ_i^+, ξ_i^- = available clearance at TL baffle in leg i in positive and negative directions, respectively
σ_{max} = maximum tube stress in the bend region

creases the curvature of the semi-circular bend) at a generic point. Y_o is the distance of the centroidal axis from the neutral axis when the curved segment is subject to pure flexure. For an annular cross section of outer radius C_o and inner radius C_i, Y_o is defined as [4]:

$$Y_o = \frac{Zr}{2} \qquad (4)$$

where

$$Z = -1 + \frac{2r}{C_o^2 - C_i^2}\left[(r^2 - C_i^2)^{1/2} - (r^2 - C_o^2)^{1/2}\right] \qquad (5)$$

ϕ (in equation 3) is the shear stress distribution factor. For thin annular cross sections ϕ can be shown to be equal to two. λ is the flexibility factor attributable to the elastic ovaling of thin walled circular cross sections of curved elements during bending. A generally accepted semi-empirical expression for λ is due to Rodabaugh and George [5],

$$\lambda = \frac{f}{1 + \frac{6p\,C_m}{Et}\left(\frac{C_m}{t}\right)^{4/3}\cdot\left(\frac{r}{C_m}\right)^{1/3}} \geq 1 \qquad (6a)$$

where

$$f = \frac{1.65\,C_m^2}{tr} \qquad (6b)$$

where t is the wall thickness of the tubing and p is the internal pressure.

Referring to Fig. 3, Castigliano's theorem requires:

$$\frac{\partial U}{\partial P} = \delta - 2r\alpha_1 - \frac{P(2\ell_s - S_1 - S_2)}{AE} \qquad (7a)$$

$$\frac{\partial U}{\partial R} = -(\epsilon_1 + \epsilon_2 - 2\Delta) + (S_1 - S_2)\,\alpha_1 \qquad (7b)$$

$$\frac{\partial U}{\partial M_2} = -(\alpha_1 + \alpha_2) \qquad (7c)$$

In nearly all texts on solid mechanics, the Castigliano's theorem is applied to an elastic system with an immovable point of reference, e.g. the built-in end of a cantilevered beam. The foregoing equations illustrate an application of this powerful principle to an elastic system undergoing elastic deformation as well as rigid body motion.

Using equations (3) and (7), after performing necessary integrations and algebraic manipulations (omitted here for brevity), three additional linear equations in α_1, α_2, R and P are obtained. α_1 is substituted out from these equations using equation (2). The resulting set of three linear equations may be written in subscript notation as

$$B_{ij}\,x_j = f_i;\ i = 1, 2, 3 \qquad (8)$$

with the implied identities $\{x\} = \{\alpha_2, R, P\}$ and $\{f\} = \{\delta, 2\Delta - \epsilon_1 - \epsilon_2, 0\}$. ϵ_1 and ϵ_2 denote outward displacements of points 0_1 and 0_2 (Fig. 3).

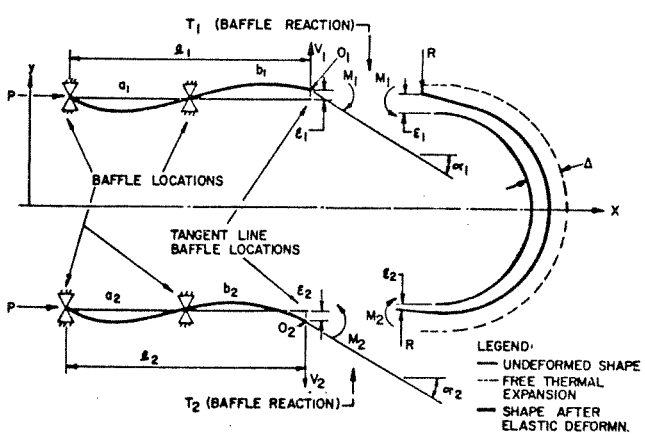

Fig. 3 Two-span model and U-bend deformation kinematics

The elements of the $[B]$ matrix are given in the Appendix for reference. Simplifying equation (8) further yields explicit expressions for R, P and α_2 as follows:

$$R = \frac{1}{D}\left[\left(B_{23} - \frac{B_{21}B_{33}}{B_{31}}\right)\delta - \left(B_{13} - \frac{B_{11}B_{33}}{B_{31}}\right)(2\Delta - \epsilon_1 - \epsilon_2)\right] \qquad (9a)$$

$$P = \frac{1}{D}\left[\left(B_{12} - \frac{B_{11}B_{32}}{B_{31}}\right)(2\Delta - \epsilon_1 - \epsilon_2) - \left(B_{22} - \frac{B_{21}B_{32}}{B_{31}}\right)\delta\right] \qquad (9b)$$

$$\alpha_2 = -\frac{1}{B_{31}}(B_{32}R + B_{33}P) \qquad (10)$$

where

$$D = \left(B_{12} - \frac{B_{11}B_{32}}{B_{31}}\right)\left(B_{23} - \frac{B_{21}B_{33}}{B_{31}}\right) - \left(B_{22} - \frac{B_{21}B_{32}}{B_{31}}\right)\left(B_{13} - \frac{B_{11}B_{33}}{B_{31}}\right) \qquad (11)$$

All unknowns in the problem can now be computed provided the rotational stiffnesses K_1 and K_2 are known. We recognize that the stiffnesses strongly depend on the adjacent spans. The influence of remote spans on K_i is minimal. Hence to develop a manageably simple expression for K_i, we consider a two-span model, as shown in Fig. 3. Referring to Fig. 3, the following relationships follow from classical beam flexure theory.

$$EI\epsilon_i = \frac{V_i\ell_i b_i^2}{3} - \frac{M_i b_i(2\ell_i + b_i)}{6} \qquad (12)$$

$$EI\alpha_i = \frac{M_i(2b_i + \ell_i)}{3} - \frac{V_i b_i(3\ell_i - a_i)}{6} \qquad (13)$$

where $i = 1 = 2$ for the two legs respectively, eliminating V_i from equations (12) and (13), we have

$$\alpha_i = \rho_i M_i - \eta_i \qquad (14)$$

where

$$\rho_i = \frac{1}{EI}\left[\frac{2b_i + \ell_i}{3} - \frac{(3\ell_i - a_i)(2\ell_i + b_i)}{12\ell_i}\right] \qquad (15a)$$

$$\eta_i = \frac{(3\ell_i - a_i)\,\epsilon_i}{2\ell_i b_i} \qquad (15b)$$

Thus, equations (1) and (14) yield the explicit expression for K_i, we have

$$K_i = \frac{1}{\rho_i} + \frac{\eta_i}{\rho_i\alpha_i} \qquad (16)$$

We note that η_i vanishes when ϵ_i is zero and K_i becomes independent of α_i. However, if a small lateral displacement at the TL baffle location is allowed (nonzero ϵ_i), then K_i becomes dependent on α_i.

Finally, the reaction at the TL baffle location is given by

$$T_i = R - V_i \qquad (17)$$

where V_i follows from equations (12) and (13):

$$V_i = \frac{3}{\ell_i b_i^2}\left[EI\,\epsilon_i + \frac{M_i b_i}{6}(2\ell_i + b_i)\right] \qquad (18)$$

The solution procedure to solve a specific problem can now be described.

3 Method of Solution

The solution is fairly straightforward for the case where the TL baffles are assumed to have zero clearance. Incidentally this is also a conservative approximation since it will result in an overestimate of the computed U-bend stresses. The rotational stiffnesses, K_i, follow from equation (16). Equations (9) and (10) yield the magnitudes of R, P and α_2 respectively. α_1 is computed with equation (2).

The computation is a bit more involved if small clearances at the

TL baffle locations are stipulated. Let ξ_i^+ and ξ_i^- denote the available clearances at leg i in the positive and negative y-directions. To determine if the tube will move and take up the clearances (say ξ_1^+ and ξ_2^-), we proceed as follows.

Step (1): Assume $\epsilon_1 = \xi_1^+$, and $\epsilon_2 = \xi_2^-$, and solve for K_i (equation 16).

Step (2): Solve for R, P and α_2 using equations (9) and (10) respectively.

Compute α_1 by equation (2).

Step (3): Compute M_i in equation (14). The corrected values of K_i are then given by $K_i' = M_i/\alpha_i$.

Step (4): If K_i' is equal to K_i within a specified tolerance (say .1 percent absolute error) then the solution is said to have converged. The values of R, P, α_i computed in Step 2 are the solution values. However, if K_i' is discrepant from K_i, then assume new K_i equal to average of the previous K_i and K_i' computed in the preceding step.

Return to Step (2).

This procedure is repeated until the solution converges. Sometimes it may require as many as eight to ten iterations.

The crucial check on whether the tube will indeed contact the baffle by undergoing the assumed lateral displacements can now be made. A physically meaningful solution requires that for non-zero ϵ_i,

$$\frac{T_i}{\epsilon_i} > 0; i = 1, 2 \tag{19}$$

If inequality (19) is not satisfied, then the assumed displacements ϵ_1 and ϵ_2 may be excessive, or in the wrong direction. If the search process for compatible ϵ_i shows that the tube does not contact the baffle hole in either positive or negative direction, then the natural inference for an intermediate displacement would require that the corresponding T_i be zero. Following the foregoing logical steps, an appropriate solution algorithm can be devised to determine the correct lateral displacements.

It is of some interest to observe that the solution is greatly complicated by the incorporation of clearances at TL baffle supports. The complication will proportionately increase if clearances at other baffle locations are also introduced. These, however, will have a much weaker influence on the U-bend stress field.

It should be noted that the rotational stiffnesses developed in the preceding section are based on a two-span beam model. Additional beam spans can be accounted for by modifying equations (12) and (13). Such refinements do not add much to the accuracy of the results.

Having determined the principal unknowns in the problem, the stress field in the U-tube is found from static equilibrium. The moment M and direct force N at a point A (Fig. 1) are given by

$$M = M_2 + R\,(S_2 + r\sin\theta) + P\,r\,(1 - \text{Cos}\theta) \tag{20a}$$

$$N = P\,\text{Cos}\theta - R\,\sin\theta \tag{20b}$$

Thus the maximum bending stress due to M is given by

$$\sigma_b = \frac{\psi M C_o}{I} \tag{21}$$

ψ is the meridional stress concentration factor associated with the ovaling of thin walled cross sections. A widely accepted expression for ψ is due to Rodabaugh, et al. [5]:

$$\psi = \frac{\psi_o}{1 + \dfrac{13p\,C_m}{4Et}\left(\dfrac{C_m}{t}\right)^{3/2}\left(\dfrac{r}{C_m}\right)^{2/3}} \geq 1 \tag{22}$$

where

$$\psi_o = \frac{0.9}{\left(\dfrac{tr}{C_m{}^2}\right)^{2/3}} \tag{23}$$

The foregoing expression for ψ is nearly half of the theoretical value derived by Clark and Reissner [6], and later refined by Cheng and Thailer [7]. The maximum stress σ_b (equation 21) is circumferential bending stress which occurs at the centroidal axis transverse to the plane of bending. Thus the longitudinal stress intensification factor is not required to compute the peak stress intensity. To perform a complete stress analysis, however, expressions for the stress intensification factors as a function of meridional angle as derived in reference [7] may be used. As mentioned before, these theoretical expressions for ψ are nearly twice as large as that given by the widely used formula of Rodabaugh, et al.

4 Example

To illustrate the solution technique and to study the effect of major design parameters we will consider a typical U-tube 0.75 in. (19 mm) OD, 16 B.W.G. (.065 in.) wall, 1.25 in. (31.75 mm) bend radius, 100 in. (254 cm) long straight legs, subject to an inter-leg differential expansion δ equal to .05 in. (1.27 mm). The radial expansion of the U-bend is .002 in. (.0508 mm). The Young's modulus of tube material is assumed to be 30×10^6 psi ($.207 \times 10^6$ MPa).

As a basic configuration we will assume that $a_i = b_i = 10$ in. (25.4 cm), $\epsilon_i = 0$ and $S_i = 1$ in. (2.54 cm) ($i = 1, 2$). We will study the effect of variation of a_1, b_i, S_i, tube radius r, tube wall and baffle location clearances ϵ_i on the stress field in the tube. The central object is to identify those parameters which are most effective in reducing tube bending stress.

The bending stress in the U-bend as a function of angular orientation θ is shown in Fig. 4 (Case A). Curves B and C correspond to overhang dimensions $S_i = 0$ and 2 in. respectively. We note that the bending stress is a rather strong function of S_i. Providing a two in. overhang on both legs of the U reduces the maximum bending stress by over 40 percent. The location of the maximum bending stress also shifts as S_i is changed. By considering equilibrium of the curved segment, it can be shown that $\sigma_{\max}$ will occur at either $\theta = 0$, π or $\theta \geq \pi/2$. Referring to Fig. 2, the moment M at an angular location θ is given by

$$M = M_2 + R\,(S_2 + r\sin\theta) + \text{Pr}\,(1 - \text{Cos}\,\theta)$$

For an extremum, we have

$$\frac{\partial M}{\partial \theta} = 0 = R\,r\cos\theta + P\,r\sin\theta$$

$$\text{or } \theta = \tan^{-1}\left(\frac{-R}{P}\right) \tag{24}$$

Furthermore, for a maximum

$$\frac{\partial^2 M}{\partial \theta^2} < 0$$

which implies

$$P\,\text{Cos}\,\theta - R\,\sin\theta < 0 \tag{25}$$

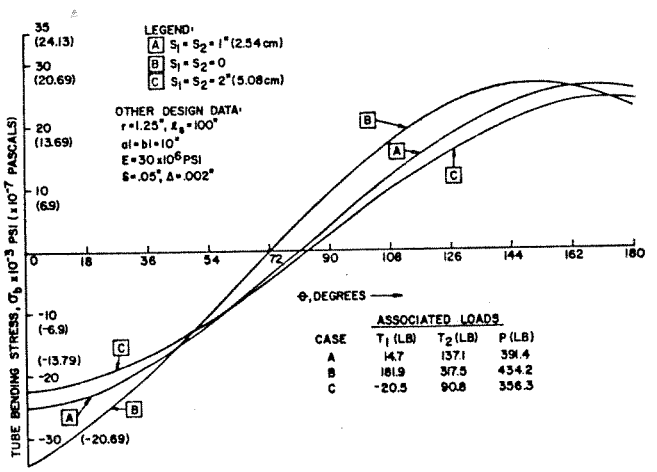

Fig. 4 Variation of circumference bending stress with angular orientation

In the above equation θ is measured from the tangent line of the leg in tension, i.e. P is assumed to be positive. Two conditions may exist:

a. Positive R: This means (equation 24) θ will lie in the second quadrant, i.e. $\pi/2 \leq \theta \leq \pi$.

Inequality (25) yields

$$\tan\theta < \frac{P}{R}$$

Substituting for $\tan\theta$, we have the requirement for a maximum:

$$P^2 > -R^2$$

This requirement is obviously satisfied for all R and P.

b. Negative R: Equation (24) requires that the maximum lie in the first quadrant, i.e. $\theta \leq \pi/2$. Inequality (25) yields

$$\tan\theta > \frac{P}{R}$$

which implies that $P^2 < -R^2$

This condition obviously cannot be satisfied. Hence negative R implies that maximum tube bending stress must occur at $\theta = 0$ or π.

Finally, it is apparent that the stresses in the U-bend can be optimized by adjusting S_1 and S_2 to make the stress variation as closely symmetrical with respect to $\theta = \pi/2$ as possible.

Table 1 shows principal quantities of interest for some selected values of ϵ_1 and ϵ_2. The remainder of the design data corresponds to the basic configuration. The maximum tube stress σ_{max} and tube axial load P are seen to be rather weakly dependent on ξ_i. This indicates that the baffle clearance at the tangent line baffle has a limited influence in mitigating tube bend stresses in typical geometrics.

Fig. 5 shows the variation of σ_{max} and P with a_i and b_i (assumed equal). Both curves are convex to the origin indicating that σ_{max} and P increase rapidly at small support spacings. Baffle spacings have a marked effect on σ_{max} and P. Increasing a_i and b_i from ten in. to 20 in. decreases σ_{max} by over 23 percent. However, there are practical limitations on the baffle spacings due to consideration of heat transfer, flow induced vibration, etc. Noting that the axial load produces tensile stresses in one leg and compressive stresses in another, the baffle spacings in the tension leg can be made larger than the compression leg while maintaining the same factor of safety against flow induced vibration. In general, adjusting a_i and b_i provides an effective tool to generate a favorable stress field in the U-tube.

Another design parameter with a profound influence in the U-bend stress field is the bend radius r. Generally r can be increased without such limitations as accompany the baffle spacings. The only drawback in increasing r is the reduction in the number of tubes that can be assembled in a given tubesheet size. Fig. 6 shows σ_{max} and P as a function of r. Both curves are convex to the origin indicating that the tube stresses rise rapidly with a decrease in the bend radius.

Table 2 contains some representative results for 3/4 in. (19 mm) and 5/8 in. (16 mm) tubing for three different tube gages. We notice that the maximum tube bending stresses increase with reduction in tube wall for 3/4 in. (19 mm) tubing. This is contrary to our general experience with thermal stresses. However this paradox is explained by

Table 1 Maximum tube stress, axial load, support reactions versus clearance at the T.L. baffle

ξ_1 In. (mm)	ξ_2 In. (mm)	P LB (N)	T_1 LB (N)	T_2 LB (N)	Max. Tube Stress, σ, PSI (M Pa)
0	0	391.4 (1740.9)	14.7 (65.4)	137.1 (609.8)	25600 (176.5)
−.004 (−.102)	.008 (.203)	376.8 (1676.)	−67.9 (−302.)	45.3 (201.5)	24916 (171.8)
−.008 (−.203)	.012 (.305)	367 (1632.4)	−64.9 (−288.7)	42.3 (188.2)	24280 (167.4)
−.022 (−.559)	.025 (.635)	334 (1485.6)	−32.9 (−146.3)	53.9 (239.7)	22016 (151.8)

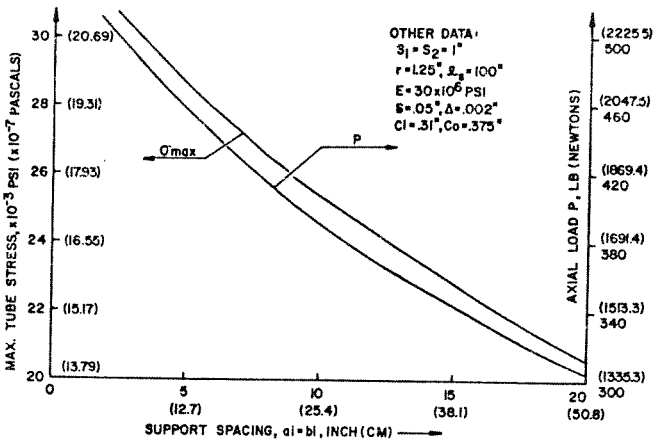

Fig. 5 Maximum tube stress σ_{max} and axial load of P versus support spacing

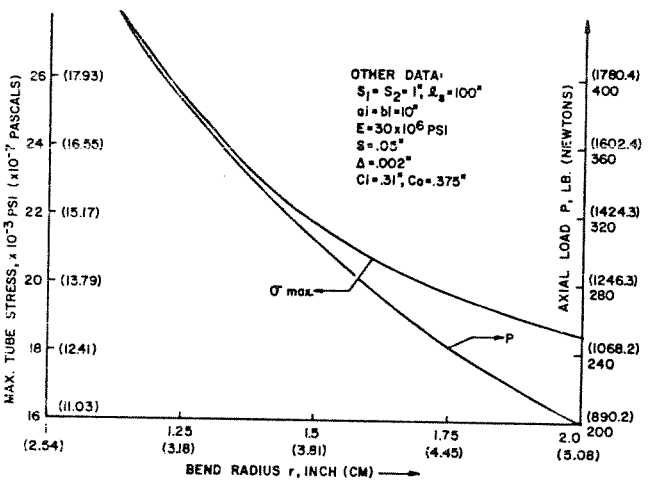

Fig. 6 Maximum tube stress σ_{max} and axial load P versus bend radius

noting that the tube stress intensification factor ψ is increased with reduction in the tube wall. Thus as the tube wall is decreased, the bending stresses are boosted by ψ and reduced by the increase in the flexibility of the system. This suggests the possibility of an optimum thickness. Observing the results for 5/8 in. (16 mm) tubing, we note that an optimum does indeed exist for this tube size in the reported range of tube gages in Table 2. The stresses corresponding to 18 BWG are the lowest. In general, the tube bending stresses increase with reduction in the tube wall in the most common working range of tube wall thickness. It should be emphasized, however, that using a smaller diameter tubing will always reduce the maximum stress as demonstrated by the numerical results in Table 2.

5 CONCLUSION

An efficient method to determine the stress field in a U-tube subject to longitudinal differential thermal expansion has been developed. The solution is valid within the realm of linear elasticity theory. It is shown, via a numerical example, that the U-bend stresses can reach dangerously high magnitudes in commonplace designs. Some design strategies to alleviate the U-bend stress were examined in depth. The effect of overhang span S_i on the tube stress was found to be considerable. On the other hand baffle clearances ξ_i at the TL baffle did not appreciably reduce the stress level in the tube in the example problem. Among other design parameters with a pronounced effect on the bend stress, tube OD and bend radius deserve special attention. Both parameters are found to have an important bearing on the peak bending stress.

An important result emerges from the study of the effect of tube

Table 2 Maximum tube stress σ_{max}, support reactions T_i and Axial Load P, versus tube OD and gage

		Tube Dimensions Outer Rad. In. (mm)	Inner Rad In. (mm)	T_1 lb (N)	T_2 lb (N)	P lb (N)	σ_{Max} PSI (M Pa)
	16 BWG	.375	.31	14.74	137.1	391.4	25550
		(9.5)	(7.8)	(65.6)	(609.8)	(1740.9)	(176.2)
3/4 in.	18 BWG	.375	.326	8.9	98.	285.2	29305
(19 mm)		(9.5)	(8.28)	(39.6)	(435.9)	(1268.6)	(202.1)
	20 BWG	.375	.34	5.9	64.8	188.6	33515
		(9.5)	(8.64)	(26.2)	(288.2)	(838.9)	(231.1)
	16 BWG	.3125	.2475	9.2	93.3	269.	23700
		(8)	(6.29)	(40.9)	(415)	(1196.5)	(163.4)
5/8 in.	18 BWG	.3125	.2635	4.3	67.	200.6	23310
(16 mm)		(8)	(6.69)	(19.1)	(298)	(892.2)	(160.7)
	20 BWG	.3125	.2775	2	44.5	136.	27180
		(8)	(7.05)	(8.9)	(197.9)	(604.9)	(187.4)

gage on the maximum bending stress intensity. The maximum tube bending stress is seen to increase with increased tube gage for 3/4 in. (19 mm) tubing (Table 2). This conclusion is at variance with the characteristic response of structures to thermal loadings. Increased structural flexibility is generally expected to reduce the maximum stress in the system. This discrepant behavior of the U-tube is readily explained by noting that the stress intensification factor ψ rapidly increases with reduction in the tube wall. Thus even though the net internal moment is reduced by increased tube flexibility, the bending stress may sustain a net increase due to the effect of the stress intensification factor. For some geometries, an optimum gage may exist which minimizes the bending stress. In the example problem, 5/8 in. (16 mm) tubing is found to have such an optimum (18 BWG).

In addition to these geometric parameters, other design alternatives to reduce the U-bend stress should be explored. For example, arranging more passes in the tubeside will decrease the net temperature change in any pair of passes thus reducing δ. U-tubes in various passes can also be made of different lengths to reduce δ in the most critical pair of tube passes connected by U-tubes. Shell-side flow arrangement also has a bearing on the U-bend differential expansion problem. It can be shown that subjecting both legs of a U-tube to the same shell stream will result in a smaller δ than the configuration where the two legs are in contact with two shell streams. Thus the U-tube differential expansion in a one shell pass-two tube pass exchanger will be less than that in a two tube-two shell pass exchanger, for an otherwise identical geometry. The heat transfer problem must be studied in conjunction with the structural problem to devise the most suitable design in a given situation.

References

1 Singh, K. P., "Analysis of Vertically Mounted Through-Tube Heat Exchangers," *Trans ASME*, JOURNAL OF ENGRG. FOR POWER, Vol. 100, No. 2, April 1978, pp 380–390.

2 Gardner, K. A., "Mean Metal Temperatures in Shell-and-Tube Heat Exchangers," A proprietary report to HTRI and TEMA, private communication, 1977.

3 Sokolnikoff, I. S., *Mathematical Theory of Elasticity*, Second Edition, McGraw Hill, New York, 1956, p. 394.

4 Seely, F. B., Smith, J. O., *Advanced Mechanics of Materials*, second edition, Wiley, New York, 1965, p. 665.

5 Rodabaugh, E. C., George, H. H., "Effect of Internal Pressure on Flexibility and Stress-Intensification Factors of Curved Pipe or Welding Elbows," *Pressure Vessel and Piping Design*, Collected Papers 1927–1959, ASME, 1960, pp. 467–476.

6 Clark, R. A., Reissner, E., "Bending of Curved Tubes," *Advances in Applied Mechanics*, Vol. 2, Academy Press, New York, 1951, pp. 93–122.

7 Cheng, D. H., Thailer, H. J., "On Bending of Curved Tubes," *Pressure Vessels and Piping: Design and Analysis*, Vol. 2, ASME, New York, 1972, pp. 1175–1179.

APPENDIX

Elements of [B] matrix

$$B_{11} = \left(\frac{\pi r^2}{EI'} + \frac{2rS_1}{EI} + \frac{2r}{K_1}\right) K_2$$

$$B_{12} = \frac{r^2}{EI'}(\pi S_2 + 2r) - \frac{rS_1}{EI}(S_1 - 2S_2) - \frac{2r}{K_1}(S_1 - S_2) - \frac{2r}{EA}$$

$$B_{13} = r^2\left\{\frac{3\pi r}{2EI'} + \frac{4S_1}{EI} + \frac{4}{K_1}\right\} + \frac{1}{EA}\left(2\ell_s - \frac{\pi r}{2}\right) + \frac{\phi \pi r}{2GA}$$

$$B_{21} = \left[\frac{(\pi S_2 + 2r)\, r}{EI'} - \frac{1}{2\,EI}\{(S_1 - S_2)^2 - 2\,S_2^2\} - \frac{2}{EA} - \frac{S_1 - S_2}{K_1}\right] K_2$$

$$B_{22} = \frac{r}{EI'}\left\{S_2(\pi S_2 + 2r) + r\left(\frac{\pi r}{2} + 2S_2\right)\right\} + \frac{1}{3\,EI}\{(S_1 - S_2)^3 + 2\,S_2^3\} + \frac{(S_1 - S_2)^2}{K_1} - \frac{\pi r}{2\,EA} - \frac{4\,S_2}{EA} + \frac{\phi\,\pi r}{2\,GA} + \frac{\Phi\,(S_1 + S_2)}{GA}$$

$$B_{23} = \frac{r^2}{EI'}(\pi S_2 + 2r) - \frac{r\,S_1}{EI}(S_1 - 2\,S_2) - \frac{2r\,(S_1 - S_2)}{K_1} - \frac{2r}{EA}$$

$$B_{31} = 1 + \frac{K_2}{K_1} + \frac{K_2\,(S_1 + S_2)}{EI} + \frac{K_2\,\pi r}{EI'}$$

$$B_{32} = \frac{1}{2\,EI}\{2\,S_2^2 - (S_1 - S_2)^2\} + \frac{r}{EI'}(\pi S_2 + 2r) - \frac{(S_1 - S_2)}{K_1} - \frac{2}{EA}$$

$$B_{33} = \frac{\pi\, r^2}{EI'} + \frac{2r}{K_1} + \frac{2r\,S_1}{EI}$$

Where $I' = \lambda A Y_0 r$.